A Hybrid Particle-Field Coarse-Grained Molecular Model for Pluronics Water Mixtures

Antonio De Nicola,* Toshihiro Kawakatsu, Giuseppe Milano*

Dedicated to Professor Gaetano Guerra and published as part of the special collection of articles celebrating his 60th birthday

In the framework of a hybrid particle-field simulation technique where self-consistent field (SCF) theory and molecular dynamics (MD) are combined, specific coarse-grained (CG) models for Pluronic block copolymers are developed. In particular, the behavior of the model in the correct reproduction of micellar and non-micellar phases has been tested for Pluronic L62 and L64. At different temperature and polymer contents of the water–polymer mixture, the proposed model is able to correctly describe the different morphologies that are experimentally found. The proposed CG models, still very close to atomistic ones, allow the reconstruction of full atomistic structures by applying suitable reverse mapping techniques. This opens the way to all atom description of these systems.

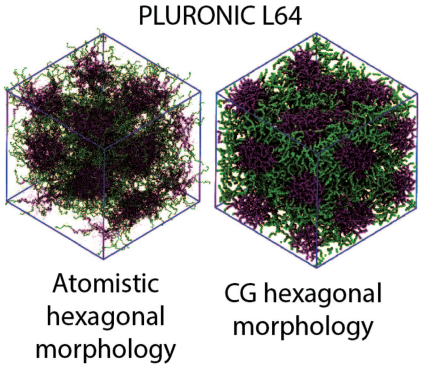

1. Introduction

The triblock copolymers of poly(ethylene oxide)$_m$–poly(propylene oxide)$_n$–poly(ethylene oxide)$_m$ (PEO$_m$–PPO$_n$–PEO$_m$) are an important family of amphiphilic polymers. They are commercially known and available as Pluronic or Poloxamer. The hydrophilic–lipophilic characters of these block copolymers can be tuned by varying the block length and the molecular weight of both PEO and PPO blocks. Such adaptability has allowed these copolymers to be employed in many fields, like foaming, detergency, dispersion stabilization, emulsification, lubrication, cosmetic formulation,[1] and surface modification for biocompatibility[2] for medical applications.[3] The Pluronic micelles used for drug delivery are one of the most studied for medical applications.[3] Such micelles have the capability to include hydrophobic drugs inside the PPO core[4] and transport them in the body. Recently, Pluronic micelles have also been used in the cancer therapy.[5] For these reasons, the micellar phase has been investigated in depth by numerous experimental techniques. For example, the critical micelle concentration (CMC) and the critical micelle temperature (CMT) have been studied by dynamic light scattering[6] and fluorescence spectroscopy.[7] Extensive experimental studies of the Pluronic phase behavior in water has been reported by Alexandridis[8–10] and Yang[11] and Chu.[12]

A study of the micellization kinetics of Pluronic L64 in water, measured by dynamic light scattering, shows that the self-assembly process is a complex multistep phenomenon that occurs on a time scale of the order of microseconds.[6]

Atomistic simulations, due to the large length and time scales involved, cannot be directly applied to study these self-assembly phenomena. Just to have an idea about

A. De Nicola, Dr. G. Milano
Dipartimento di Chimica e Biologia, Università di Salerno, I-84084 via Ponte don Melillo Fisciano (SA), Italy
E-mail: adenicola@unisa.it; gmilano@unisa.it
A. De Nicola, Dr. G. Milano
IMAST Scarl-Technological District in Polymer and Composite Engineering, P. le Bovio 22, 80133 Napoli (NA), Italy
Prof. T. Kawakatsu
Department of Physics, Tohoku University, Aoba, Aramaki, Aoba-ku, Sendai 980-8578, Japan

DOI: 10.1002/macp.201300214

the size, if we consider a simulation of 300 Pluronic L62 chains hydrated by 56 000 water molecules, which is, the smallest system studied in the present work, it would involve about 200 000 particles. Atomistic simulations, due to their computational costs, are usually confined to systems on time and length scales of nanoseconds and few nanometers.

On the other hand, different computational approaches based on mean field density functional theory have been proposed for these systems.[13,14] Fraaije and co-workers[15] proposed a model to study the morphologies of nondilute water–Pluronic solutions. In the framework of self-consistent field (SCF) theory, the model systems are not represented by particles, but by density fields, and the mutual interactions between the segments are decoupled and replaced by interactions between the segments and static external fields. Such approaches are computationally less expensive and reach time and length scales able to reproduce the morphologies of different phases. Their disadvantage is that in such models the chemical specificity and the link with atomic structure are difficult to achieve.

A different approach, based on reference atomistic data, using a coarse-grained (CG) implicit solvent model has been reported by Bedrov and co-workers,[16,17] whereas a similar CG model for symmetric triblock copolymers, but having explicit water beads, has been reported by Hatakeyama and Faller.[18] Such CG models are computationally less expensive compared with atomistic models, but are still expensive compared with SCF approaches and are of quite limited use for the investigation of the formation of phase patterns.

We present a computational study of the phase behavior of binary Pluronic–water mixtures, based on the hybrid particle-field (PF) molecular dynamics (MD) method.[19,20] The idea behind the hybrid PF-MD approach is to obtain a strategy, as far as will be possible, having a similar accessibility to large time and length scales of pure SCF methods, and including, at the same time, the chemical specificity of atomistic and CG models. Recently, PF models of phospholipids[21,22] have been reported to study the phase behavior of phospholipid–water mixtures. Such models have shown the possibility of reaching large time and length scales, comparable with SCF approaches, and keeping, at the same time, chemical specificity.

In particular, we investigate the phase behavior as function of the composition and temperature for the Pluronics PEO_6–PPO_{34}–PEO_6 (L62) and PEO_{13}–PPO_{30}–PEO_{13} (L64).

At a low polymer concentration in a water solution, Pluronic chains self-assemble in micellar phases. The micelles are formed by a hydrophobic core, mainly composed of PPO blocks, and by a hydrophilic corona formed by hydrated PEO blocks. At higher polymer wt% content, the Pluronic chains self-assemble in different phases, passing through the lamellar phase to isotropic solutions at high polymer contents.[8,23–25]

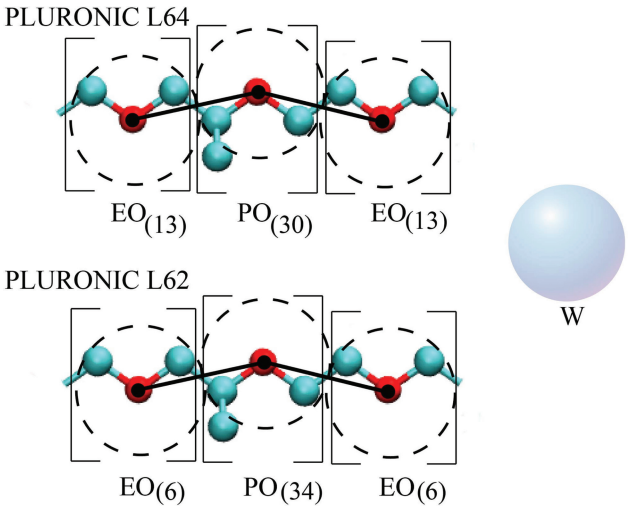

Figure 1. The mapping scheme used for the model of Pluronic. Each EO bead corresponds to three heavy atoms. For PO, each bead corresponds to four heavy atoms. The effective beads are centered on oxygen atoms (depicted in red) for both EO and PO types. The bead type W corresponds to four real water molecules.

Table 1. Parameters for bond potential represented by Equation 3.

Bond type	r_{bond} [nm]	K_{bond} [kJ mol^{-1} nm^{-2}]
PEO – PEO	0.28	8000.00
PPO – PPO	0.28	5000.00
PEO – PPO	0.28	6500.00

Table 2. Parameters for angle potential represented by Equation 4.

Angle type	θ [°]	K_θ [kJ mol^{-1}]
PEO – PEO – PEO	155.00	40.00
PEO – PPO – PPO	140.00	40.00
PEO – PEO – PPO	140.00	30.00
PPO – PPO – PPO	140.00	30.00

The aim of this work is to present and validate the CG model for micellar and non-micellar phases. In particular, the transferability of the model to systems at different polymer contents has been investigated.

The paper is organized as follows: Section 2 will briefly describe the basic concepts of hybrid PF-MD. In addition, in the same section, the model and the computational details will be given. In Section 3, results will be discussed,

and finally the reproduction of the phase behavior of the model will be described.

2. Computational Method

The main feature of the hybrid PF-MD approach is that the evaluation of the nonbonded force and its potential between atoms of different molecules can be replaced by the evaluation of an external potential, which depends only on the local density at position r in the PF simulations. According to the spirit of the SCF theory, a many body problem like molecular motion in many molecule systems can be reduced and treated like a problem of deriving the partition function of a single particle in an external potential $V(r)$. Non-bonded force between atoms of different molecules can be obtained from a suitable expression of the potential $V(r)$ and its derivatives.

In the framework of SCF theory, a molecule is regarded to be interacting with the surrounding molecules, not directly, but through a mean field.

We assume that the interacting potential W depending on the density takes the following form:

$$W\left[\{\phi_K(\mathrm{r})\}\right] = \int d\mathrm{r}\left(\frac{k_BT}{2}\sum_{KK'}\chi_{KK'}\phi_K(\mathrm{r})\,\phi_{K'}(\mathrm{r}) + \frac{1}{2\kappa}\left(\sum_K \phi_K(\mathrm{r}) - 1\right)^2\right) \quad (1)$$

where each component species is specified by the index K, and $\phi_K(r)$ is the CG density of the species K at position r. The term $\chi_{KK'}$ is the mean field parameter for the interaction of a particle of type K with the density fields due to particles of type K', while k is the compressibility, which is assumed to be sufficiently small, and ϕ_0 is the total number density of segments (we assume that the volume for all segments is the same).

Table 3. PF interaction matrix. $\chi_{KK'}$*RT [kJ mol^{-1}].

	Water	PEO	PPO
Water	0.00	1.50	4.60
PEG	1.50	0.00	16.00
PPO	4.60	16.00	0.00

It can be shown that using the so-called saddle point approximation, the external potential is given by:

$$V_K(\mathrm{r}) = \frac{\delta W\left[\{\phi_K(\mathrm{r})\}\right]}{\delta\phi_K(\mathrm{r})} = k_BT\sum_{K'}\chi_{KK'}\phi_K(\mathrm{r}) + \frac{1}{\kappa}\left(\sum_K \phi_K(\mathrm{r}) - 1\right) \quad (2)$$

The main advantage of the hybrid PF-MD scheme is that the most computationally expensive part of the MD simulations, the evaluation of the nonbonded force between atoms of different molecules, is replaced by the evaluation of forces between single molecules with an external potential. Connecting the particle and field models is necessary to obtain a smooth CG density function directly from the particle positions. This function is obtained by implementing a mesh-based approach, which is also suitable to obtain the density derivatives needed to calculate the forces. The details of the implementation of this approach and a complete derivation of Equation 2 are described in refs.[19,20] The simulations

Table 4. Simulated system.

Systems	Composition (no. of molecules)				Polymer [wt%]	Temp. [K]	Box size [nm]	Simulated time [μs]
	L62	L64	Water	Particle no.				
I	304	0	56 016	70 000	20	303	20 × 20 × 20	2.7
II	791	0	33 614	70 000	52	303	20 × 20 × 20	3.3
III	1065	0	21 010	70 000	70	303	20 × 20 × 20	3.5
IV	1370	0	6980	70 000	90	303	20 × 20 × 20	3.5
V	0	250	56 000	70 000	20	303	20 × 20 × 20	3.5
VI	0	650	33 600	70 000	52	303	20 × 20 × 20	3.7
VII	0	875	21 000	70 000	70	303	20 × 20 × 20	4.3
VIII	0	1125	7000	70 000	90	303	20 × 20 × 20	3.3
IX	0	1	8500	8556	24	303[a)]	10 × 10 × 10	0.3
X	0	3696	23 000	230 000	90	303	30 × 30 × 30	6.0

[a)]System IX was also simulated at temperatures of 288, 293, and 298 K.

reported here were performed using the parallel version of the OCCAM code.[26]

2.1. Model and Parameters

The CG model used in this study is parameterized on the basis of the results of atomistic models reported by some of us in a previous paper.[27] Moreover, we tested the reproduction of the structural properties of a single micelle of Pluronic L64 compared with the experimental data.[28]

The model of Pluronic employed in this study can be considered to be an extension of the GC model reported in ref.,[29] from which the bonds and angle distributions have been used to parametrize the intramolecular interactions. Different from the models already reported, in the framework of PF models, here, the intermolecular interactions have been evaluated using a field theoretic approach.[19,20]

The mapping scheme adopted for the CG model in the present work is depicted in Figure 1. Each bead of the CG model for EO and PO corresponds to three (C−O−C) and four [C(CH_3)−O−C] heavy atoms, respectively. Oxygen atoms (depicted in red in Figure 1) were considered as centers of each bead for both EO and PO repeating units. According to this, the bond length between two beads corresponds to the distance between two oxygen atoms of the two consecutive repeating units. The angle formed between two adjacent vectors corresponds to angle formed between three consecutive oxygen atoms of three consecutive monomers. The target distributions of bond and angle are calculated from atomistic simulations.[27]

The force-field parameters of the CG model, for the intramolecular part, were taken from previous papers.[27,29] Such a CG force field is based on the reproduction of both bond and angle distributions of atomistic simulations,[27] in which small oligomers of PEO and PPO have been simulated in water and different solvents. Force-field parameters for intramolecular interactions are summarized in Table 1 and 2. In particular, the bond is described by a harmonic potential of the form:

$$V_{\text{bond}}(r) = \frac{1}{2}K_{\text{bond}}(r - r_{\text{bond}})^2 \quad (3)$$

where r_{bond} is the equilibrium bond length and K_{bond} is the force constant.

The stiffness of the chains is also taken into account by a bending potential $V_{\text{angle}}(\theta)$, which depends on the cosine of the angle θ between two successive bonds:

$$V_{\text{angle}}(\theta) = \frac{1}{2}K_{\text{angle}}\{\cos(\theta) - \cos(\theta_0)\}^2 \quad (4)$$

where K_{angle} is the force constant and θ_0 is the equilibrium bond angle. Angle parameters adopted for the models in this paper are reported in Table 2.

The PF parameters (Equation 2) $\chi_{KK'}$ required to calculate the interactions between a particle of type K and the density field due to the particles type K' are listed in Table 3.

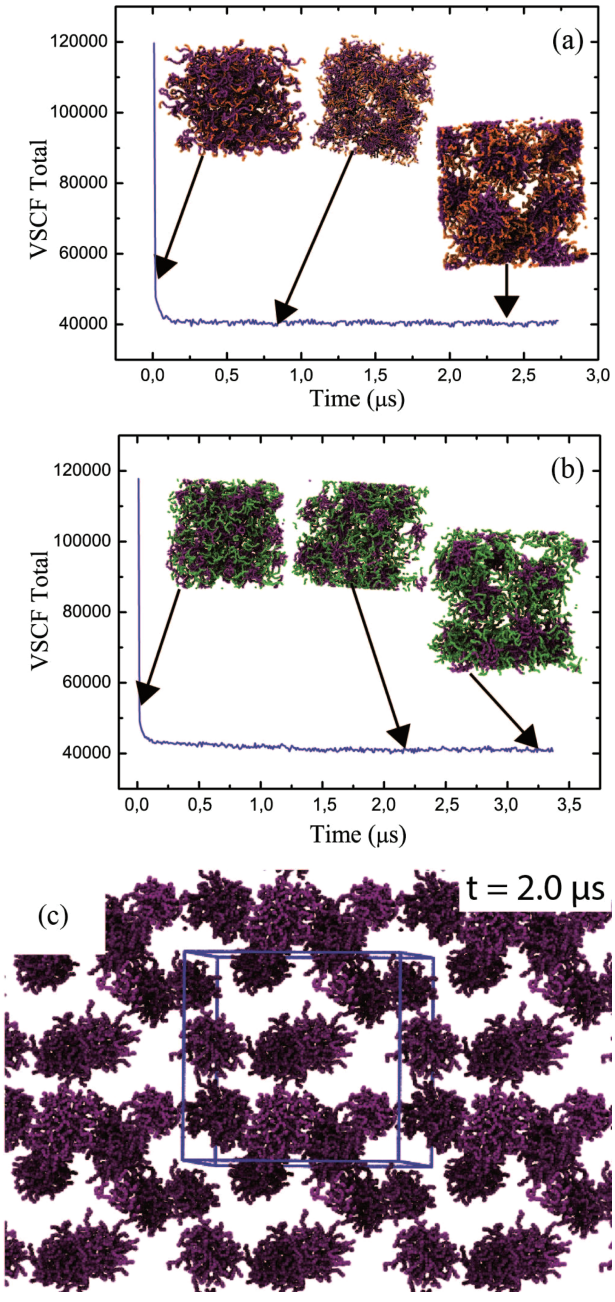

Figure 2. Time behavior of SCF potential for the composition of 20 wt% polymer content. a) System I of Pluronic L62. b) System V of Pluronic L64. c) Representative snapshot of the micellar phase in which the system has been extended in the *xy* plane. Only the hydrophobic PPO blocks are depicted. The different colors, orange and green, assigned to the PEO beads of Pluronic L64 and L62 have been assigned to enable the L62 and L64 to be easily distinguished in the snapshots of the simulations. No differences in the mapping scheme or interaction parameters exist. The water beads W are omitted for clarity.

The PF interaction parameters between PEO–water and PPO–water have been tuned to reproduce the radius of gyration in aqueous solutions of the PEO and PPO polymers, at different molecular weights.[28]

2.2. Computational Details

The parallel program OCCAM[26,30] was used for the MD simulations. All of the simulations were performed using a time step of 0.03 ps, with an *NVT* ensemble, by keeping the temperature constant using an Andersen thermostat with a collision frequency of 7 ps^{-1}. The grid density was updated every 300 steps. Details of the systems composition and size used in the present work are summarized in Table 4.

3. Results and Discussion

In principle, the parameters of a CG model are not easily transferable. In particular, the $\chi_{KK'}$ parameters required to calculate the interactions between a particle of type K and the density field due to the particles type K' can depend on composition and temperature. This dependency cannot be known a priori and need to be investigated for every CG model.

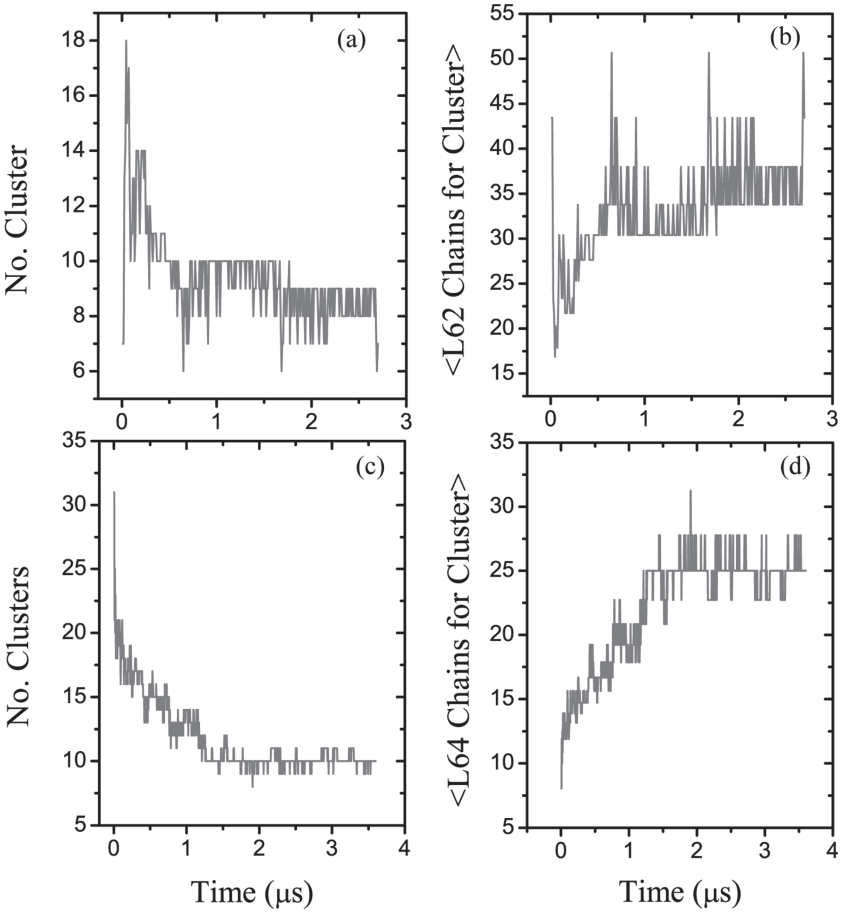

Figure 3. Time behavior of: a) number of Pluronic L62 clusters for the system I. b) Number of Pluronic L62 chains per cluster for the system I. c) Number of Pluronic L64 clusters for the system V. d) Number of Pluronic L64 chains per cluster for the system V. The number of clusters is calculated on the basis of a cut-off value (1 nm) on the shortest distance between PPO units of two different L64 chains.

The main purpose of the present work was to study and validate the PF model for both micellar and non-micellar phases corresponding to low and high block-copolymer contents, respectively. In particular, two different block copolymers, Pluronic L62 and Pluronic L64, were chosen. Although the molecular weights of Pluronic L62 and L64 are comparable (≈2900), the ratio of PEO:PPO is quite different, and consequently the hydrophobic–lipophilic balance (HLB), which summarizes the structural differences, assumes values of 7 for L62 and 15 for L64.[31] The HLB is defined as the ratio of the lengths of the EO on PO blocks. It can be expressed by the following empirical form:[31,32]

$$\mathrm{HLB} = -36.0\frac{N_{\mathrm{PO}}}{N_{\mathrm{PE}} + N_{\mathrm{PO}}} + 33.2 \quad (5)$$

We investigate a binary block copolymer–water system of both Pluronic L62 and L64 to observe the spontaneous formation of different morphologies as a function of concentration and temperature. To this aim, four different polymer concentrations were considered (polymer contents of 20, 52, 70, and 90 wt%).

3.1. Micellar and Hexagonal Phases

The time behavior of the SCF potentials (Equation 2) of the systems at different concentrations is reported in Figure 2. Representative snapshots of the systems are included above the plots. The compositions of the simulated systems are reported in Table 4. At low Pluronic concentration (20 wt%), in agreement with the experimental phase behavior,[8] a micellar morphology was found. At that concentration, the block-copolymer molecules self-assemble into spherical micelles for both L62 and L64 (Figure 2a,b). The micellar phase reproduction is not surprising because the model used in this work was parameterized at a similar concentration and tuned to reproduce the experimental

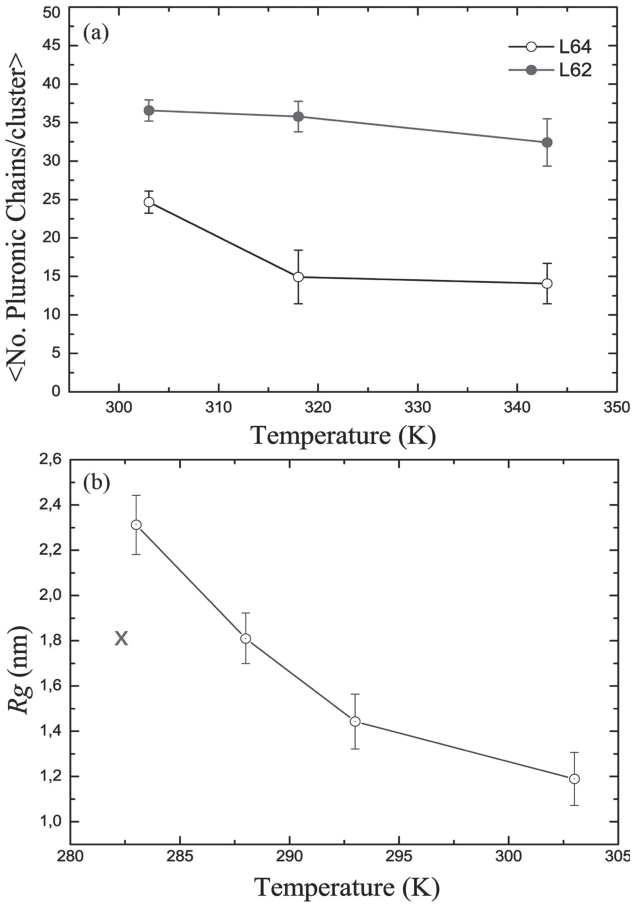

Figure 4. a) Average number of Pluronic chains per cluster depending on the temperature for both L62 and L64. b) Radius of gyration of a L64 single chain in water, calculated at different temperatures (system IX). The red cross represents the experimental value.[40]

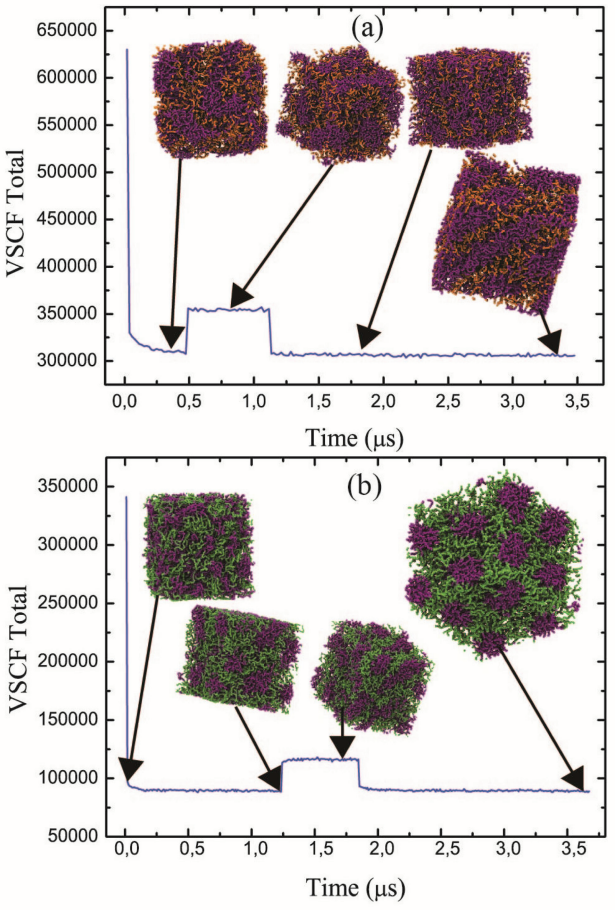

Figure 5. Time behavior of the SCF potential for the composition of 52 wt% polymer content. a) System II of Pluronic L62. b) System VI of Pluronic L64.

radii, of core and corona, of an L64 micelle. In Figure 2c, a representative snapshot of micellar phase is reported. To favor the visualization, the system has been extended in the one plane.

The time behaviors of both the number of clusters and the number of chains per cluster (i.e., aggregation number, N_{agg}) are reported in Figure 3. From the plots, it is clear that, starting from 2 μs for both L62 and L64, the number of clusters and the aggregation number fluctuate around a constant value. The time needed for the formation of stable micellar structures is of the same order of magnitude as that reported from experiments.[33,34]

The temperature dependence of the cluster size was also investigated. The calculated N_{agg} = 24 at 303 K is comparable to the experimental value of 19 found at the same temperature.[35] As reported by Alexandridis and coworkers[36] for a diluite solution of Pluronic L64 (2.5 wt%), N_{agg} increases from 37 to 54 in the temperature range 37–55 °C. In a nondilute water/L64 solution (31.9 wt%), an increase of N_{agg} from 1 up to 69 in the temperature range 8–35 °C has been reported by Wu et al.[37] A similar behavior of the temperature dependency of N_{agg} has been found for different Pluronics, P85,[23,35] F88, F68, and F127.[35]

As pointed out by Alexandridis et al.,[36] the hydrophobic block of the Pluronic is responsible for the micellization due to the diminishing hydrogen bonding between the water and the PPO with increasing temperature. Correspondingly, the PEO–water and PPO–water χ interaction parameters increase with tempereature[38] and the PEO–PPO interaction parameter decreases.[39]

We found a different behavior for our model; in fact, as shown in the Figure 4a, the average number of Pluronic L64/cluster decreases by increasing the temperature. The same behavior was found for the Pluronic L62. The origin of this disagreement between experiments and simulations can be ascribed to the use of fixed $\chi_{KK'}$ parameters at different temperatures. A better agreement

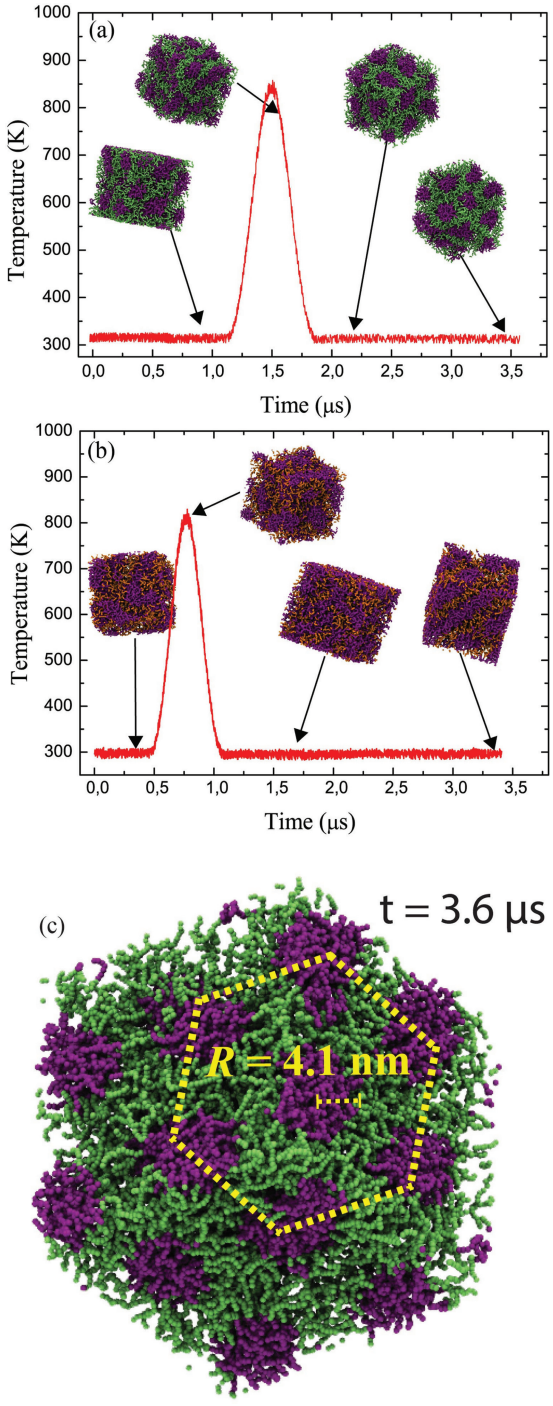

Figure 6. Temperature–time behavior: a) System VI Pluronic L64 forming a hexagonal morphology. b) System II Pluronic L62 forming a lamellar morphology. c) Detail of hexagonal morphology obtained for the Pluronic L64. The experimental value[42] of apolar cylinder radius R is reported in the picture.

could be obtained using a more-flexible model, allowing the correct temperature dependency of $\chi_{PEO,W}$ and $\chi_{PPO,W}$ (of the type $\chi = \chi_0\left(A_1 + \frac{B_1}{T}\right)$) and of $\chi_{PEO,PPO}$ (of the type $\chi = \chi_0\left(A_2 + \frac{B_2}{T}\right)$), where A_i and B_i can be tuned to reproduce the correct experimental behavior.

In addition, the radius of gyration (R_g) of a single L64 chain in water has been calculated at different temperatures, and the results have been compared with the experimental value.[40] In Figure 4b, the temperature behavior of R_g is reported. The red cross represents the experimental value of R_g measured by light scattering for a water solution of Pluronic L64 with a concentration below the CMC. We found, for our model at 283 K, a value of R_g of 2.3 nm, larger than the experimental one (1.8 nm).[40] Also in this case, temperature-dependent χ parameters would lead to a better agreement.

The experimental phase diagram[41] of both Pluronic L62 and Pluronic L64 shows that the morphologies corresponding to the phases in the range of 50–80 wt% are different for L62 and L64. In particular, for the Pluronic L62, the lamellar morphology is stable in the range of 60–70 wt%. Differently, the Pluronic L64, having a similar PPO block to that of L62 but longer PEO blocks, shows the presence of an additional hexagonal phase, which is rather narrow and extends from 46 to 52 wt% L64 content. Although the wt% content of the system II for the Pluronic L62 is not representative of a hexagonal phase, we studied that composition for both L62 and L64 to test the specificity of our model in the reproduction of this peculiar phase behavior.

In Figure 5a,b, the time behaviors of the SCF potential are reported. To speed up the self-assembly process, an annealing procedure was applied for both Pluronics. The systems were heated up to 830 K and cooled down to 303 K in about 0.6 μs for both. Then, the temperature of the systems was kept constant, using an Andersen thermostat, at 303 K. The temperature–time behaviors, together with significant snapshots of the systems, are reported in Figure 6a,b. For the Pluronic L62, according to the experimental phase behavior, the hexagonal morphology is not obtained. Differently, for the Pluronic L64, a hexagonal morphology, according to experimental phase diagram,[41] is reached after 2.1 μs. In that phase, the PO chains self-assemble in cylindrical structures with a well-defined periodicity. A structural parameter of the hexagonal morphology, depending on the periodicity, is the apolar cylinder radius (R) of the PPO block. In Figure 6c, it is clear that the simulated structure well agrees with the experimental value of $R = 4.1$ nm reported by Alexandridis et al.[8]

3.2. Lamellar Phase and High-Polymer-Content Isotropic Solution

According to the phase diagram, the composition of 70 wt% of polymer was chosen for both Pluronics. In Figure 7a,b,

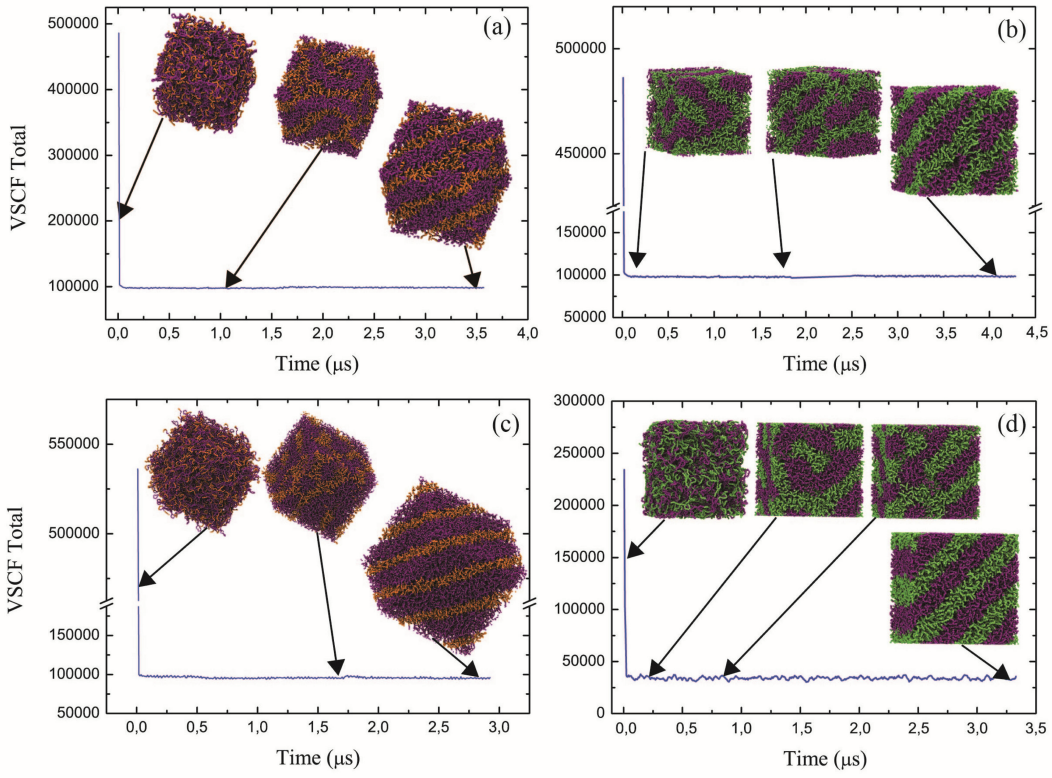

Figure 7. Time behavior of the SCF potential for compositions of 70 and 90 wt% polymer content. a) System III of Pluronic L62. b) System IV of Pluronic L64. c) System VII of Pluronic L62. d) System VIII of Pluronic L64.

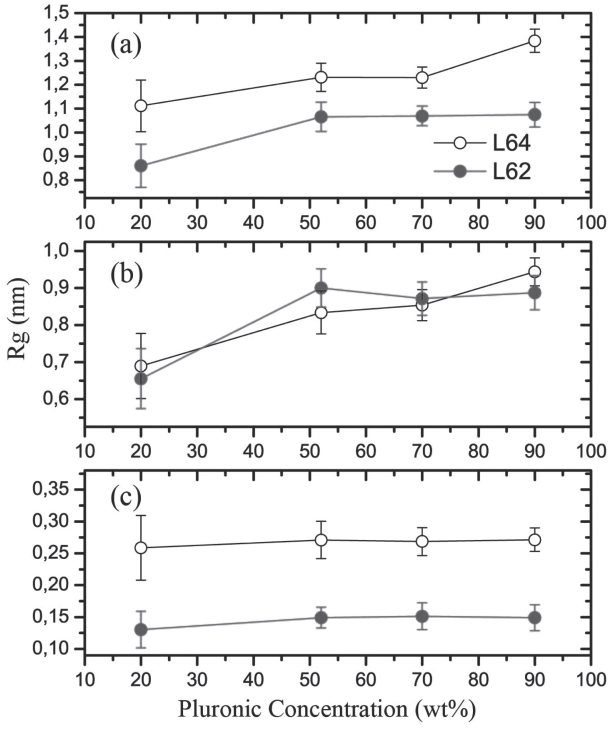

Figure 8. Average R_g, depending on the wt% polymer content, of: a) total chain of Pluronic, b) the PPO block, c) the PEO blocks. The empty black circle represents the Pluronic L64. The red whole circle is used for the Pluronic L62.

time behavior of the SCF potential is reported. During the simulations, the SCF potential quickly reaches an equilibrium, and a well-structured lamellar morphology, according to the experimental behavior,[8] was found for both Pluronic L62 and L64. We also extended the investigation of phase-behavior reproduction of our model in the phase with polymer contents higher than 70 wt%. To this aim, the composition of 90 wt% of polymer was chosen. In Figure 7c,d, the time behaviors of the SCF potential are reported for both Pluronics. For the L62, we obtain, at equilibrium, a lamellar morphology instead of complex interconnected structures, as postulated from the experiments. Similarly, for the Pluronic L64, we obtained a morphology close to the lamellar one, but with defects. Probably, these results are affected by finite size effects, due to the periodic boundary conditions (PBC) favoring the lamellar morphologies.

The behavior of R_g as a function of polymer composition was also investigated. In particular, we report in Figure 8 the R_g of the entire chain of PO and the partial R_g calculated for PEO and PPO segments separately. As expected, the high water content of the systems I and V plays a strong role in the PPO segregation, resulting in the smallest R_g found for all composition studied. Instead, at higher block copolymer contents, we observe an increase of the total R_g and PPO. A significant variation of R_g of the PEO blocks was not observed (Figure 8c).

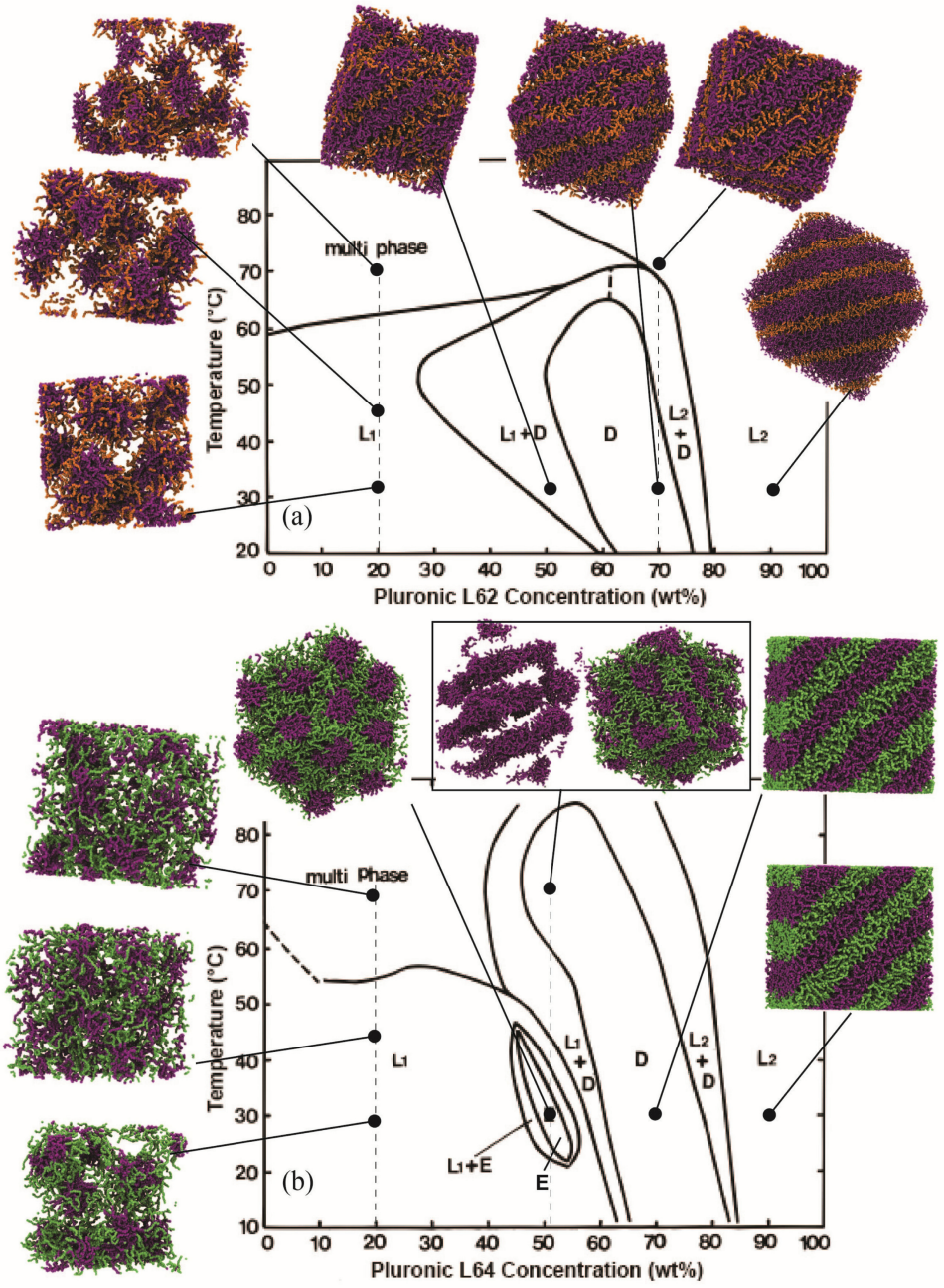

Figure 9. Phase diagrams for Pluronic L62 (a) and Pluronic L64 (b). For any composition and temperature studied, a snapshot of the obtained morphology is depicted in the diagram. The phase diagrams are redrawn from ref.[8]

All the morphologies obtained at different contents of polymer and different temperatures for both Pluronic L62 and L64 together with the experimental-phase diagram are depicted in Figure 9.

For the Pluronic L62, the morphologies found at 303 K are in agreement with the experimental-phase diagram.[8] In fact, at low polymer content, we found a spherical micellar morphology, as expected. A lamellar morphology was observed at Pluronic L62 contents of 52, 70, and 90 wt%, as expected. Differently from the phase diagram, for the 90 wt%, we still found the lamellar morphology instead of complex interconnected structures.

For the Pluronic L64, a similar figure has been shown. At 303 K, we found micellar, hexagonal, and lamellar morphologies according to phase diagram.[8] At temperatures higher than 303 K, we found a stable micellar morphology for 20 wt% of L64. Instead, at 52 wt%, the hexagonal morphology is not stable, according to phase

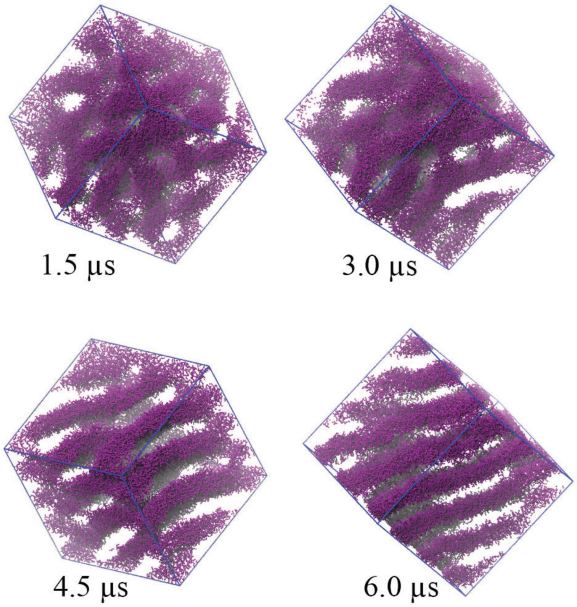

Figure 10. Snapshots of the system X (see Table 4) taken at different time. The box lengths is 1.5 times (30 × 30 × 30 nm) larger than used for the other systems studied in the present work.

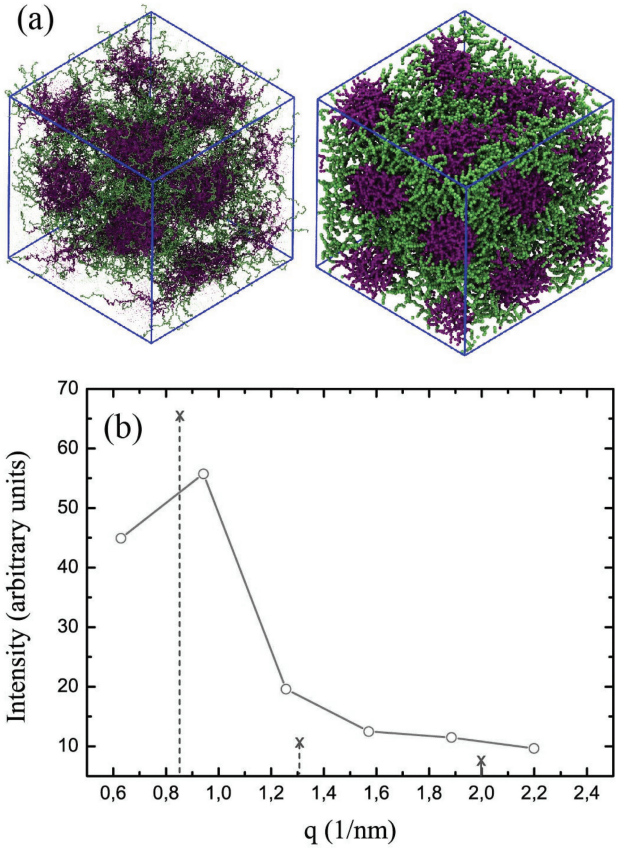

Figure 11. a) Atomistic structure, obtained after reverse mapping procedure, and CG structure of the hexagonal morphology for the Pluronic L64. Each EO or PO bead corresponds to three or four heavy atoms, respectively. b) Calculated scattering intensities, as function of the wave number (q), for the atomistic structure of hexagonal morphology obtained for the Pluronic L64. The blue points represent the experimental values of the SAXS spectra.[8]

diagram, and a lamellar morphology with defects has been observed.

At an L64 content of 90 wt%, as observed for L62, we found a lamellar morphology instead of the more complex structures postulated from experiments. Probably, as discussed above, the simulation results are affected by finite size effects due to the PBC favoring lamellar morphologies. To reduce such effects, we simulated a system in which the box lengths were increased by a factor 1.5 (system X in Table 4). In Figure 10, snapshots at different times for system X are depicted. The water beads and the PEO blocks are excluded from the snapshots. Complex and interconnected structures start to be formed at 1.5 and 3.0 μs. The system evolves, in 6 μs, into a morphology having interconnected lamellae formed by PPO blocks. These complex structures, probably, are characterized by lengthscales of the same order as the box size, and further investigations with systems larger than those studied in the present work should be considered.

One of the important uses of CG models is to obtain well-relaxed structures useful for generating configurations at a higher level of chemical detail. An example is the generation, by local relaxation, of the structure of dense polymer melts at the atomistic level starting from mesoscale models.[43,44]

The Pluronic CG model presented in this work is based on atomistic models, as described in the computational method section. The mapping scheme proposed for that model is strictly connected to the atomistic scale. In fact, every EO or PO bead includes three or four heavy atoms, respectively. Differently from Pure SCF or dissipative particle dynamics (DPD)[45] approaches, our model is still very close to an atomistic one. Such a feature allows the atomistic details to be reintroduced by reverse mapping procedures.

Moreover, as shown previously, we are able to obtain morphology patterns typical of the mesoscale length. Combining the possibility of our model to reintroduce atomistic detail with morphologies obtained from the CG model on the scales of microseconds and nanometers, we report an example of reverse mapping for the hexagonal morphology. The full atomistic configuration obtained was formed from ≈600 000 particles. In Figure 11a, both atomistic and CG structures are depicted. From the atomistic structure, the scattering intensities as function of the wave number (q) are calculated and compared with the SAXS spectrum,[8] as shown in Figure 11b.

4. Conclusion

A hybrid PF-MD CG model has been reported for Pluronic L62 and L64. The reproduction of morphologies depending on the concentration and temperature for water mixture solutions of polymer has been tested. In particular, micellar and non-micellar morphologies reproduced by the model have been found in agreement with the experimental-phase diagram. Furthermore, the reproduction of the hexagonal morphology specific for the Pluronic L64 has been obtained. In fact, in a narrow range of composition, between 46 and 55 wt%, the hexagonal phase is stable for the Pluronic L64, and, at the same composition, is absent in the Pluronic L62 phase diagram.

At polymer contents higher than 52 wt%, we obtain a lamellar morphology for both L62 and L64. In particular, at 90 wt% of L64, we also observe a complex lamellar morphology.

The features of the proposed model allow the possibility of linking the CG configurations to the full atomistic configurations due to 1:3 and 1:4 mappings for the EO and PO beads. An example of reverse mapping of the peculiar hexagonal morphology of Pluronic L64 has been shown to this aim.

To have an idea about simulations reported in this paper, for systems X of Table 4, it is possible to calculate about 0.5 μs in 1 day using 32 processors (Intel E5530). The hybrid PF-MD approach is particularly efficient in parallel simulations, especially for large systems when the use of a large number of CPUs is efficient.[26] The validation of the models presented in this paper will allow their application to large-scale systems.

Acknowledgements: G.M. and A.D.N. thank MIUR (FIRB "RETE ITALNANONET") for financial support and the HPC team of ENEA (http://www.enea.it) for using the ENEA-GRID and the HPC facilities CRESCO (http://www.cresco.enea.it) in Portici, Italy.

Received: February 20, 2013; Published online: June 17, 2013; DOI: 10.1002/macp.201300214

Keywords: coarse-grained; molecular dynamics; phase behavior; Pluronic; SCF

[1] I. R. Schmolka, *J. Am. Oil Chem. Soc.* **1977**, *54*, 110.
[2] M. Amiji, K. Park, *J. Biomater. Sci., Polym. Ed.* **1993**, *4*, 217.
[3] A. V. Kabanov, E. V. Batrakova, V. Y. Alakhov, *J. Controlled Release* **2002**, *82*, 189.
[4] B. Foster, T. Cosgrove, B. Hammouda, *Langmuir* **2009**, *25*, 6760.
[5] C. Peetla, A. Stine, V. Labhasetwar, *Mol. Pharm.* **2009**, *6*, 1264.
[6] W. Brown, K. Schillen, M. Almgren, S. Hvidt, P. Bahadur, *J. Phys. Chem.* **1991**, *95*, 1850.
[7] N. J. Turro, B. H. Baretz, P. L. Kuo, *Macromolecules* **1984**, *17*, 1321.
[8] P. Alexandridis, D. Zhou, A. Khan, *Langmuir* **1996**, *12*, 2690.
[9] P. Alexandridis, V. Athanassiou, T. A. Hatton, *Langmuir* **1995**, *11*, 2442.
[10] P. Alexandridis, J. F. Holzwarth, T. A. Hatton, *Macromolecules* **1994**, *27*, 2414.
[11] S. Yang, S. Yuan, X. Zhang, Y. Yan, *Colloids Surf. A* **2008**, *322*, 87.
[12] Z. Zhou, B. Chu, *Macromolecules* **1987**, *20*, 3089.
[13] D.-W. Li, X. Y. Liu, Y. P. Feng, *J. Phys. Chem. B* **2004**, *108*, 11206.
[14] H. Liu, Y. Li, W. E. Krause, M. A. Pasquinelli, O. J. Rojas, *J. Phys. Chem.* **2012**, *4*, 87.
[15] B. A. C. van Vlimmeren, N. M. Maurits, A. V. Zvelindovsky, G. J. A. Sevink, J. G. E. M. Fraaije, *Macromolecules* **1999,** *32,* 646.
[16] D. Bedrov, C. Ayyagari, G. D. Smith, *J. Chem. Theory Comput.* **2006**, *2*, 598.
[17] G. D. Smith, D. Bedrov, J. Yoon, *Langmuir* **2007**, *23*, 12031.
[18] M. M. Hatakeyama, R. R. Faller, *Phys. Chem. Chem. Phys.* **2007**, *9*, 4662.
[19] G. Milano, T. Kawakatsu, *J. Chem. Phys.* **2009**, *130*, 214106.
[20] G. Milano, T. Kawakatsu, *J. Chem. Phys.* **2010**, *133*, 214102.
[21] A. De Nicola, Y. Zhao, T. Kawakatsu, D. Roccatano, G. Milano, *J. Chem. Theory Comput.* **2011**, *7*, 2947.
[22] A. De Nicola, Y. Zhao, T. Kawakatsu, *Theor. Chem. Acc.* **2012**, *131*, 1167.
[23] K. Mortensen, J. S. Pedersen, *Macromolecules* **1993**, *26*, 805.
[24] A. Caragheorgheopol, S. Schlick, *J. Phys. Chem.* **1998**, *31*, 7736.
[25] Z. Zhou, B. Chu, *Macromolecules* **1994**, *27*, 2025.
[26] Y. Zhao, A. De Nicola, T. Kawakatsu, G. Milano, *J. Comput. Chem.* **2012**, *33*, 868.
[27] S. Hezaveh, S. Samanta, G. Milano, D. Roccatano, *J. Chem. Phys.* **2011**, *135*, 164501.
[28] A. De Nicola, Y. Zhao, S. Hezaveh, T. Kawakatsu, D. Roccatano, *unpublished.*
[29] S. Hezaveh, S. Samanta, A. De Nicola, G. Milano, D. Roccatano, *J. Phys. Chem. B* **2012**, *116*, 14333.
[30] OCCAM molecular dynamics simulator, https://www.molnac.unisa.it/occam, G. Milano, accessed June 2013.
[31] M. Y. Kozlov, N. S. Melik-Nubarov, E. V. Batrakova, A. V. Kabanov, *Macromolecules* **2000**, *33*, 3305.
[32] E. Batrakova, S. Lee, S. Li, A. Venne, V. Alakhov, A. Kabanov, *Pharm. Res.* **1999**, *16*, 1373.
[33] M. J. Kositza, C. Bohne, P. Alexandridis, T. A. Hatton, J. F. Holzwarth, *J. Am. Chem. Soc.* **1999**, *15*, 322.
[34] M. J. Kositza, G. D. Rees, A. Holzwarth, J. F. Holzwarth, *J. Am. Chem. Soc.* **2000**, *16*, 9035.
[35] P. Alexandridis, T. Alan Hatton, *Colloids Surf. A* **1995**, *96*, 1.
[36] L. Yang, P. Alexandridis, D. Steytler, M. Kositza, J. Holzwarth, *Langmuir* **2000**, *16*, 8555.
[37] G. Wu, B. Chu, D. K. Schneider, *J. Phys. Chem.* **1995**, *99*, 5094.
[38] P. Linse, *Macromolecules* **1994**, *27*, 6404.
[39] M. Malmsten, B. Lindman, *J. Phys. Chem.* **1992**, *25*, 5440.
[40] B. Chu, *Langmuir* **1995**, *11*, 414.
[41] H.-X. Zhou, G. Rivas, A. P. Minton, *Annu. Rev. Biophys.* **2008**, *37*, 375.
[42] P. Alexandridis, D. Zhou, A. Khan, *J. Am. Chem. Soc.* **1996**, *12*, 2690.
[43] G. Santangelo, A. Di Matteo, F. Müller-Plathe, G. Milano, *J. Phys. Chem. B* **2007**, *111*, 2765.
[44] P. P. Carbone, H. A. H. Karimi-Varzaneh, F. F. Müller-Plathe, *Faraday Discussions* **2009**, *144*, 25.
[45] J. Pong, G. Xu, Y. Tan, *Colloid. Polym. Sci.* **2012**, *290*, 953.